J. ENVIRON. SYS., Vol. 2(4), pp. 311-337, December, 1972

The Raman Effect and Air Pollution Measurements

S. LEDERMAN
Professor
Aerospace and Applied Mechanics
M. H. BLOOM
Dean of Engineering
Director Gas Dynamics Laboratory
Polytechnic Institute of Brooklyn
Preston R. Bassett Research Laboratory
Farmingdale, N.Y.

ABSTRACT

The application of Raman scattering to air pollution detection monitoring and measurement is considered. Some theoretical as well as practical aspects of the problem are discussed. Positive as well as negative features of the Raman scattering diagnostic techniques are pointed out. The problems associated with the utilization of lasers, the power requirements, frequency selection, pulse repetition rate, and reliability are discussed. It is concluded that the diagnostic technique utilizing Raman scattering has sufficient outstanding features to make it particularly suitable for the task at hand.

Introduction

It is generally recognized that pollution of the environment on a global scale represents one of the most serious hazards confronting modern society. This pollution ranges from poor quality air in most urban

*This research was partially supported through the Center for Urban Environment Studies at P.I.B. and partially by the New York State Science and Technology Foundation under Grant No. SSF(70)-4. The authors wish to acknowledge the cooperation of Dr. P. Khosla and Mr. J. Bornstein in preparing this work.

doi: 10.2190/AKH0-NQ9L-4F9G-14Y2
http://baywood.com

communities to increasingly contaminated rivers and lakes everywhere, from nerve-wracking noise levels in many cities and towns to increasingly contaminated oceans and seashores. From recent innumerable pronouncements of ecologists, it became clear that means and methods have to be found to eliminate or at least reduce environmental pollutants generated by our advanced technological civilization if life as we know it is to survive. To accomplish this, methods and techniques have to be devised to diagnose, measure, and monitor contaminants, not only in the environment, but also at their source of generation.

In this work the problem of air pollution and, in particular, the aspect of measurement monitoring and control is being examined. Based upon surveys of available methods and techniques, it is clearly of extreme importance to have a method which would permit a remote quantitative analysis of air samples which are not easily accessible, a method which would permit three-dimensional mapping of concentrations of a number of constituents of the atmosphere simultaneously, continuously, and instantaneously. Such a method may be possible utilizing the Raman effect. As pointed out later, the diagnostic method based upon the Raman effect could provide several outstanding features. Among these would be the single-ended remote sampling ability, simultaneous and almost instantaneous identification of specific components of a mixture, quantitative analysis of a mixture, and the ability of spatial and time resolution of concentration of given components of a mixture. In this work an attempt is being made at evaluating the feasibility of obtaining quantitative data of air pollutants utilizing the Raman effect.

Nomenclature

A	attenuation	g	multiplicity
a	radius of transmitting mirror	h	Planck's constant
		I	intensity
C_1	constant $\frac{2^7\pi^5}{135}$	i	current
		k	Boltzmann constant
C_2	constant of optical system	L	optical losses
c	speed of light	m	index of refraction
ΔD	depth	N	noise
E	electronic system gain; electric field	n	number of part/cm^3
		P	dipole moment
e	electron charge	R	distance from scattering center
F	fraction of the scattered photons	r	radius of receiving mirror
Δf	bandwidth	S	signal

S_{ph} phototube sensitivity
t time
V volume in cm^3
α' isotropic part of polarizability change
β scattering coefficient
γ' anisotropic part of polarizability change
θ scattering angle
λ wavelength
μ reduced mass
ν Raman wave number shift $[cm^{-1}]$
ν_o incident wave number $[cm^{-1}]$
τ transmitivity
χ fraction of anisotropic intensity in the Q-branch

SUBSCRIPTS

A Anti-Stokes
a atmospheric absorptions
B background
b background current; absorption
d dark current
g gate
ph phototube
R Rayleigh
S Stokes
s Scattering signal
incident

The Raman Effect

The Raman effect, known for the last half century, has been discussed extensively in literature. This effect has been treated by classical as well as quantum mechanical methods and is well-documented both theoretically and experimentally. The reader might be referred to further extensive references, in particular, to References 1-5 at the end of this article. However, for the sake of completeness, a short qualitative description of this effect is given here, including some of the features which make this effect particularly suitable for this special application. When a photon of arbitrary energy encounters a molecule, the resulting collision may be of the elastic or inelastic kind. In both cases, the molecule undergoes a double transition, by first absorbing and then emitting a photon. In the case of an elastic collision, the emitted photon is of the same energy as the absorbed photon, and the resulting scattered radiation is of the same frequency as the incident radiation. In the case of inelastic collision, the energy of the re-emitted photon is changed resulting in a change in frequency of the re-emitted radiation. The former kind of scattering is known as Rayleigh scattering, while the latter as Raman scattering. This effect can be easily understood by referring to a simplified molecular energy level diagram as shown in Figure 1. Here the two photon processes responsible for the Stokes and Anti-Stokes lines as well as for the Rayleigh line are shown. The Anti-Stokes line intensity is, under normal conditions, much smaller than the Stokes lines. This is so

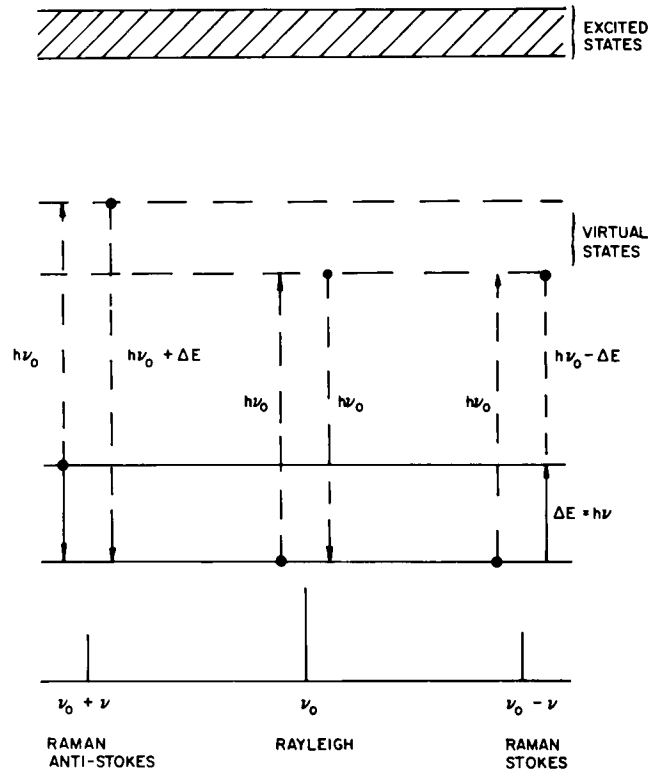

Figure 1. Energy level diagram of Raman and Rayleigh scattering.

because the number of molecules in the excited state, n, the initial state of the Anti-Stokes line is

$$N_n \sim N_m e^{-\frac{\Delta E}{kT}}$$

where N_m is the number of molecules in initial state m. The frequency shift of the scattered radiation from the incident radiation frequency is a unique characteristic of the scattering molecules and is independent of the incident radiation frequency. This property of the Raman effect affords not only an excellent possibility of distinguishing between different species of a gas mixture, but by measuring the scattered radiation intensity of each component, permits one to determine the concentration of each diatomic or polyatomic specie in the gas mixture, providing the species are Raman active. As is well-known, the Raman frequency displacements agree exactly with the

frequencies of the vibrational bands in the near infrared for those gases for which both have been observed. The Raman spectrum can, therefore, be regarded in those cases as the infrared spectrum shifted into the visible or ultraviolet region. It must, however, be noted that not all Raman active molecules are infrared active, and not all infrared active molecules are Raman active. Since in asymmetrical molecules every normal vibration is associated with a change of the dipole moment, all normal vibrations of such a molecule are infrared active. Symmetrical molecules, on the other hand, may have vibrations during which the change of the dipole moment is zero, and therefore, those molecules are infrared inactive.

In the case of the Raman spectra, the amplitude of the dipole moment induced by the incident radiation must change during the vibration considered. According to Placzek's polarizability theory, the amplitude of the induced dipole moment is given by

$$|P| = \alpha\ |E| \tag{1}$$

where α is the polarizability and E the electric field vector of the incident radiation of frequency, ν. In an asymmetric molecule, during all normal vibrations, a periodic change of the polarizability takes place, the induced dipole moment changes and the molecules are, therefore, Raman active. For symmetrical molecules, this is not always the case, although it is possible for a linear symmetrical molecule to be infrared inactive and Raman active. The linear symmetric molecule of CO_2, for example, is infrared inactive in its first normal vibration ν_1, but Raman active, and the same molecule is infrared active for ν_2 and ν_3 and Raman inactive for these vibrations. At this point, it is worthwhile noting that all homonuclear diatomic molecules like H_2, N_2, O_2 are infrared inactive, while they are all Raman active. This is one of the very important properties of the Raman effect and makes the application of the Raman effect to monitoring and measuring of air pollutants feasible, by providing a known reference for calibration purposes as will be discussed later. This description of the Raman and infrared activity of the molecular spectra is only of a very fundamental nature. For a detailed treatment of the subject, References 1 and 2 should be consulted.

The correlation between the incident radiation intensity I_o and the Raman scattered intensity, I, is given according to the polarizability theory of Placzek, including the factors introduced by the optics of the system as a function of direction θ for the Stokes and Anti-Stokes lines by

$$\frac{I_{SA\theta}}{I_o} = C_1 \frac{hnV}{8\pi^2\mu c} \frac{(\nu_o \mp \nu)^4 \{(45\alpha'^2 + 7\chi\gamma'^2)(1 + \cos^2\theta) + 6\gamma'^2\chi\sin^2\theta\} C_2}{\nu \left(1 - \exp\left[-\frac{hc\nu}{kT}\right]\right) R^2} \tag{2}$$

Equation (2) reduces to

$$\frac{I_S}{I_o} = C_1 \frac{hnV}{8\pi^2\mu c} \frac{(\nu_o - \nu)^4 \cdot 2(45\alpha'^2 + 7\chi\gamma'^2)}{\nu\left(1 - \exp - \frac{hc\nu}{kT}\right) R^2} C_2 \tag{3}$$

for backscattering (e. i., θ=180°) or for vertically polarized incident radiation and transverse observation.

The ratio of the Stokes and Anti-Stokes line intensity is given, using the Boltzmann distribution for the molecules at the appropriate energy levels by

$$\frac{I_S}{I_A} = \frac{(\nu_o - \nu)^4}{(\nu_o + \nu)^4} \exp\left(\frac{hc\nu}{kT}\right) \tag{4}$$

and the ratio of intensity of the Stokes and Rayleigh scattered radion by

$$\frac{I_S}{I_R} = \frac{(\nu_o - \nu)^4}{\nu_o{}^4} \frac{(45\alpha'^2 + 7\chi\gamma'^2)}{(45\alpha^2 + 7\chi\gamma^2)} \frac{h}{8\pi^2\mu\nu} \tag{5}$$

The temperature dependence of the Raman intensity as indicated by the exponential in the denominator of Equation (2) is shown in Figure 2. The

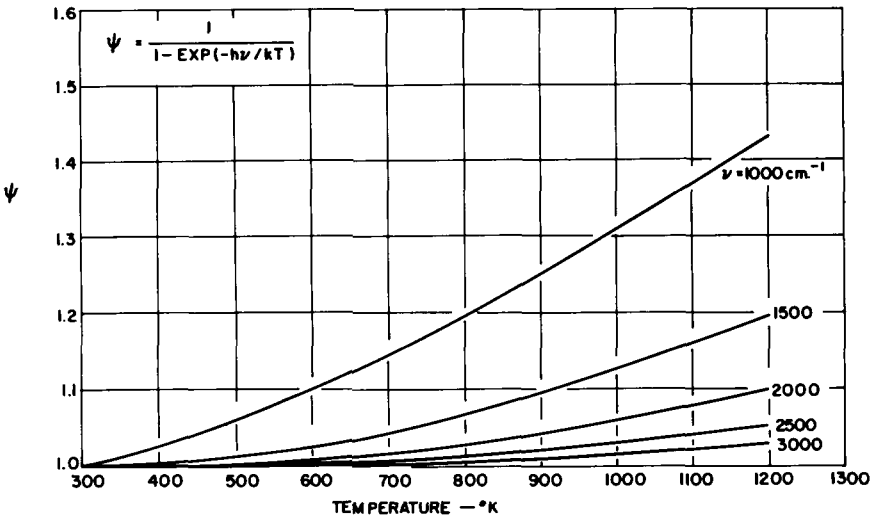

Figure 2. Temperature dependence of the Raman intensity. Raman frequency shift as a parameter.

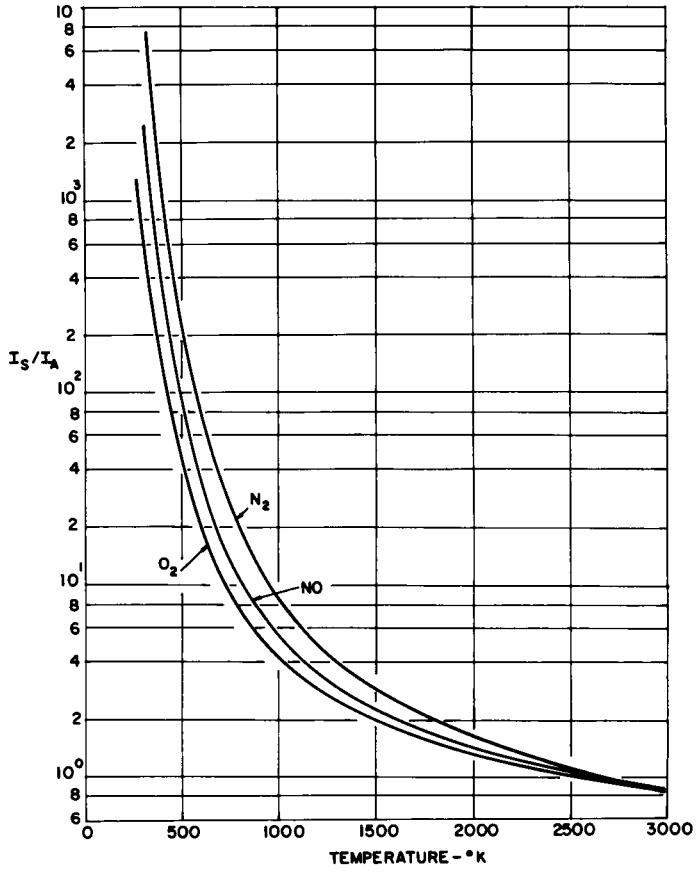

Figure 3. Ratio of the Stokes to Anti-stokes intensity as a function of gas temperature.

ratio of the Stokes to Anti-Stokes intensity for several species of interest is shown in Figure 3 and the ratio of the Rayleigh to Stokes intensity for a number of species is shown in Table 1. From these it is apparent that:

1. At room or normal atmospheric temperatures, the Stokes-Raman lines are almost independent of the temperature.
2. At normal atmospheric temperatures, the intensity of the Anti-Stokes Raman lines is very much smaller than the Stokes lines.
3. The Rayleigh line intensity is much higher than the Stokes Raman line. This will require in any application of the Raman scattering technique the utilization of band elimination filters to stop the Rayleigh line.

Table 1. Stokes to Rayleigh Intensity

Specie	$I_S/I_R \cdot 10^{-3}$ Theory	Experiment
O_2	1.9	1.93
N_2	1.32	1.19
CO_2	1.13	0.57
CH_4	3.29	2.92

One of the very important features of the Raman scattering diagnostic techniques is the ability to utilize it for range and depth resolution. The former can be accomplished by utilizing radar techniques, the latter by laser pulses and proper gates following the detector circuitry. The depth resolution ΔD can be presented as

$$\Delta D = \frac{c}{2} = (t_o + t_g) \tag{6}$$

Since, as indicated above, the Raman effect is almost instantaneous, the depth resolution appears to be governed by the laser pulse duration t_o and the gate width t_g.

Some of the more outstanding features of the Raman effect, making it suitable for the task of monitoring, measuring, and ranging of air pollutants remotely and instantaneously can thus be summarized as follows:

1. Raman scattering is very specific. Each diatomic or polyatomic Raman active specie has its own characteristic frequency shift.
2. The Raman frequency shift is independent of the illuminating frequency. This permits the choice of a convenient illuminating frequency of the incident light.
3. The Raman spectrometric system can be made single-ended; that is, the transmitter and receiver can be located in close proximity to each other.
4. The Raman diagnostic technique can be utilized for range finding. Here the highly developed radar techniques appropriately modified can be utilized. This, together with the specificity and depth resolution, permits one to determine a three-dimensional distribution of a given specie or number of species simultaneously.
5. The Raman scattered radiation from a given specie is essentially independent of the presence of other species in the volume under diagnosis. The rescattering being predominantly of the Rayleigh kind, which again accounts for a very small fraction of the incident

radiation, can, for the most part, be neglected or at most, a small correction factor introduced.

6. Since the Raman effect takes place in a time of the order of 10^{-14}, 10^{-15} sec. for an illuminating frequency in the visible or near u°v, any product of relaxation, chemical reaction or chemical production of a transient nature can be followed utilizing the Raman effect.

The Major Air Pollutants

It is generally accepted that air pollution in its broader form is a consequence of life itself. Any living creature by its mere existence contributes to the pollution of its environment. Air-breathing creatures, including man, continually add to the pollution of the air. Nature, to sustain life, must be self-cleaning. A substantial part of the pollutants, natural or man-made, are dispersed, dissolved, react among themselves and with others, chemically or physically and are thus removed from the atmosphere, either by reaching a sink such as the oceans or receptors such as plants, animals or man. As the production of pollutants increases with the population expansion and increased industrial and technological activities, the natural process of self-cleaning is not sufficient, resulting in a steadily deteriorating air environment.

The composition of clean, dry air is shown in Table 2, reproduced from

Table 2. Composition of Clean, Dry Air Near Sea Level

Component	*% by volume*	*ppm*
Nitrogen	78.09	780900.
Oxygen	20.94	209400.
Argon	0.93	9300.
Carbon Dioxide	0.0318	318.
Neon	.0018	18.
Helium	.00052	5.2
Krypton	.0001	1.0
Xenon	.000008	0.008
Nitrous Oxide	.000025	.25
Hydrogen	.00005	.5
Methane	.00015	1.5
Nitrogen Dioxide	.0000001	0.001
Ozone	.000002	.02
Sulfur Dioxide	.00000002	.0002
Carbon Monoxide	.00001	.1
Ammonia	.000001	.01

Reference 6. The average in ppm of the major air pollutants found in six U.S. cities is given in Table 3. As is evident from these tables, the content

Table 3. Summary of Concentration of Four Gases in U.S. (1962-1965 in ppm)

	1962	*1963*	*1964*	*1965*
CO_2				
Chicago	x	8.2	12.1	17.1
Cincinnati	x	7.0	6.1	4.0
Denver	x	x	x	7.2
Philadelphia	x	x	7.1	8.1
San Francisco	x	5.4	5.2	x
St. Louis	x	x	6.3	6.5
Washington	5.3	7.0	5.6	3.7
NO				
Chicago	0.104	.097	.100	.096
Cincinnati	.031	.032	.038	.031
Denver	x	x	x	.033
Philadelphia	.040	.046	.045	.048
San Francisco	.055	.087	.089	x
St. Louis	x	x	.036	.026
Washington	.029	.038	.033	.033
NO_2				
Chicago	.043	.041	.046	.043
Cincinnati	.030	.030	.032	.035
Denver	x	x	x	.036
Philadelphia	.039	.038	.038	.036
San Francisco	.033	.049	.056	x
St. Louis	x	x	.033	.026
Washington	.030	.034	.036	.034
SO_2				
Chicago	.108	.15	.175	.130
Cincinnati	.033	.025	.038	.030
Denver	x	x	x	.021
Philadelphia	.086	.069	.082	.085
San Francisco	x	.009	.017	x
St. Louis	x	x	.064	.047
Washington	.055	.046	.048	.046

of the major air pollutants is substantially higher than the air which is classified as clean. In some instances, some of these major air pollutants approach, on the average, the level where they may have adverse effects on life and vegetation. Under special, unfavorable weather conditions local concentrations may approach the emergency level, that is, the level at which it is likely that sickness or death in sensitive groups of persons may occur. The major contributors to air pollution are listed in Table 4, together with the most toxic pollutants. The above is of necessity only a very superficial review of the subject. For more detail, References 6 and 7 should be consulted, which provides a substantial list of available literature on the subject.

Table 4. National Air Pollutant Emission, 1965
(In millions of tons per year)

	Total	*% of Total*	*CO*	*SO_2*	*NO*	*Particulate Matter*	*Hydro-carbons*
Automobiles	86	60	66	1	6	1	12
Industry	23	17	2	9	2	6	4
Electrical power generation	20	14	1	12	3	3	1
Heating fuels	8	6	2	3	1	1	1
Refuse disposal	5	3	1	1	1	1	1

Design Considerations of the Apparatus

As indicated in this report, there are a number of components in the air which qualify as pollutants. Their abundance varies over a wide range. The presence of some of these components are counted in terms of hundreds of particles per million (CO_2) and are considered harmless, whereas others may become harmful when their presence amounts to .25 particles per million (NO_2 or NO).

The apparatus must, therefore, be capable of recognizing and measuring large as well as small concentrations of pollutants in the atmosphere. Since the apparatus has to function in the atmospheric environment, the atmospheric propagation properties must be considered. A complete description of the atmospheric effects on laser signal propagation is beyond the scope of this work. As is well-known, atmospheric attenuation can be described by the exponential law of attenuation. Thus the atmospheric transmitivity can be expressed as

$$\tau_a = \exp(-\alpha_a R) \tag{7}$$

where τ can be expressed as the product of the absorption and scattering transmitivities

$$\tau_a = \tau_b \cdot \tau_s \tag{8}$$

Since atmospheric absorption is generally due to the molecular constituent such as water, carbon, dioxide ozone, etc., it varies drastically with the wavelength of the illuminating light, in conformity with the molecular absorption of the given constituent. There are certain frequency bands which are completely absorbed and thus unsuitable for atmospheric probing. Some major absorption bands due to water and carbon dioxide falling in the near infrared region make utilization of infrared spectroscopy for the measurement of some pollutants impossible. The simple exponential transmission law is not applicable in absorbing regions, because of the rapid change of attenuation coefficient with wavelength. In selecting the operating wavelength for the apparatus in question, this feature must be considered.

The attenuation due to scattering, although frequency-dependent, can be described analytically and is given by Reference 8 as

$$A = A_o \exp[-R(\beta_o + \beta)] \tag{9}$$

where β, the scattering coefficient, is given by

$$\beta = \frac{32\pi^3}{3n\chi^4} (m-1)^2 \tag{10}$$

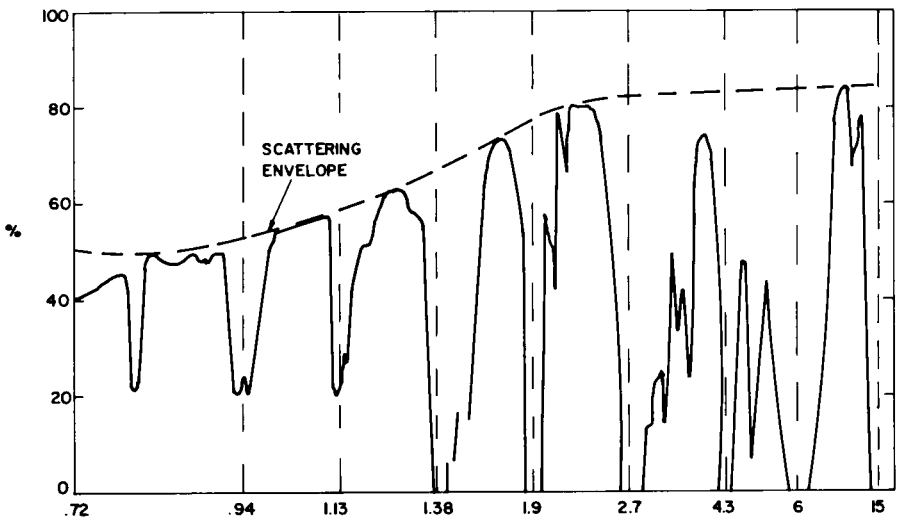

Figure 4. Transmitivity of the atmosphere.

and n equals the number of scatterers per unit volume; m denotes the index of refraction of the medium.

In Equation (9), the attenuation of the transmitted beam is given by β_0 and the attenuation of the Raman shifted radiation by β. In Figure 4, a schematic diagram of the transmitivity of the atmosphere as a function of wavelength is shown. Here, several absorption bands as well as the scattering envelope is shown. In Figures 5 and 6, the scattering coefficient β as a function of wavelength of the radiation with temperature and pressure as parameters is shown. The index of refraction m for air was used in both figures. From the last two figures it is evident that the attenuation

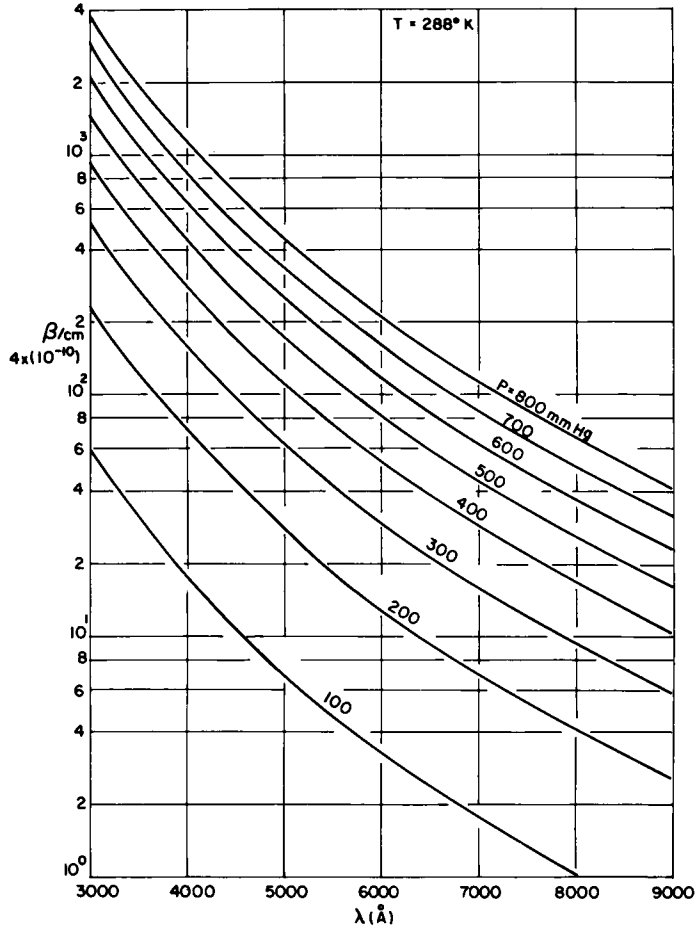

Figure 5. Scattering coefficient as a function of wavelength at constant temperature with pressure as a parameter.

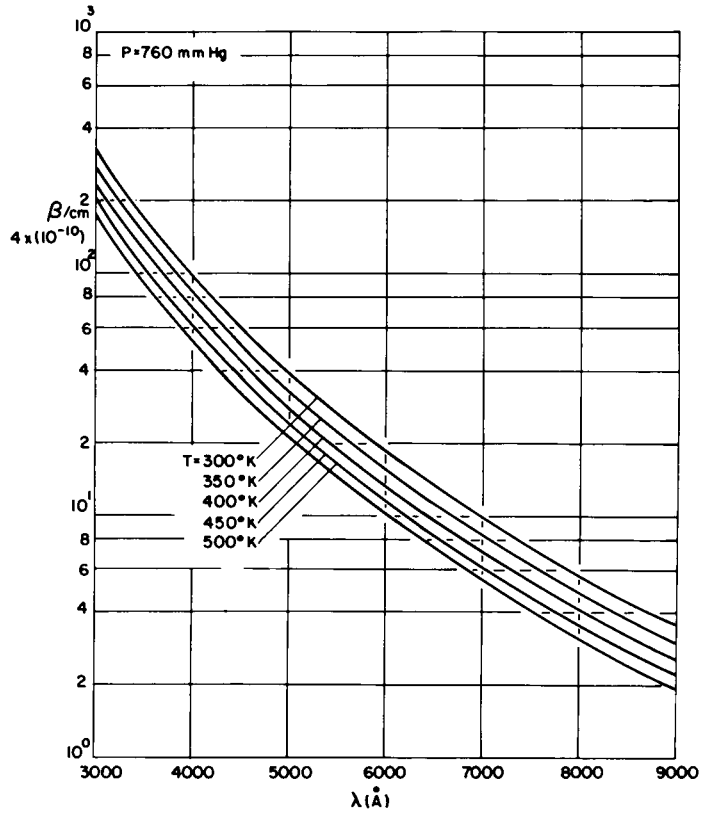

Figure 6. Scattering coefficient as a function of wavelength at constant pressure with temperature as a parameter.

of the incident as well as of the scattered radiation is not only dependent on the pressure and radiation wavelength but also on the temperature of the medium. It was found experimentally that the atmospheric attenuation coefficient due to scattering is also strongly affected by the time of the year as well as the general visibility conditions. This is shown in Figure 7, where the attenuation coefficient is plotted against wavelength for several atmospheric conditions.

The temperature fluctuations in the atmosphere also cause pockets or sheets of warmer, less dense air to mix turbulently with surrounding cooler air. Since the index of refraction of air depends upon its temperature, the interaction of a laser beam with a turbulent atmosphere leads to random amplitude and phase variation of the laser beam. The consequences of atmospheric turbulence on laser propagation may be summarized as follows:[9]

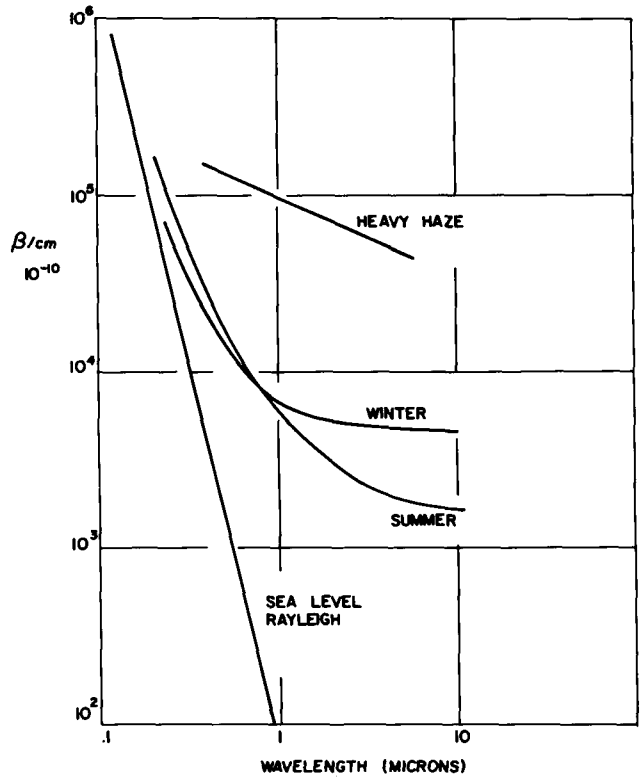

Figure 7. Atmospheric scattering coefficients for several conditions as a function of wavelength.

a. Beam steering-angular deviation of the beam from the line of sight path.

b. Variation in the beam arrival angle.

c. Beam spreading-small angle scattering increasing the beam divergence and decreasing the power density of the target.

d. Beam scintillation-small scale destructive interference.

e. Spatial coherence degradation.

f. Polarization fluctuations.

The above features would seem to present unsurmountable difficulties. This, however, is not so, The utilization of a parallel channel for normalization does provide a solution.

Inspection of Equation (3) reveals that the scattered signal is proportional to:

1. the number of scatterers in the volume being diagnosed;
2. the 4th power of the shifted frequency of the primary radiation;
3. the intensity of the primary radiation;
4. the inverse square power of the distance from the scatterers to the receiver;
5. the particular constants of the species under investigation;
6. the optics of the apparatus and electronics involved in signal processing as expressed by the constant of the system C_2 which includes also the effect of attenuation of the Raman signal on its way to the receiver.

The desired signal at the end instrument as indicated in Equation (3) depends among others on the constant C_2 which encompasses a variety of factors. It is quite obvious that the signal received will be proportional to the fraction of the scattered photons received, the atmospheric attenuation, the losses of the optics involved, the gain of the phototubes and the electronic processing of the signals received. The constant C_2 can thus be represented as:

$$C_2 = P \cdot A \cdot L \cdot E \tag{11}$$

In Equation 11, the factor P is given by

$$P = \frac{\pi r^2}{4\pi R^2} \tag{12}$$

where r is the radius of the collecting mirror or lens and R is the distance from the scattering volume. A substitution of Equation (11) into Equation (3) results in

$$\frac{I_S}{I_o} = C_3 \mathcal{R} b^2 n \frac{r^2}{R^2} \cdot A \cdot L \cdot E \tag{13}$$

where

$$C_3 = \frac{2^7 \pi^5}{135} g(45\alpha'^2 + 7\chi\gamma'^2)$$

$$\mathcal{R} = \frac{(\nu_o - \nu)^4}{\nu} \left[1 - \exp\left(-\frac{hc\nu}{kT}\right)\right]^{-1}$$

$$b^2 = \frac{h}{8\pi^2 \mu c}, \quad A = A_o \exp\left[-R(\beta + \beta_o)\right]$$

The intensity of the Raman scattered radiation as expressed by the last

equation is thus a product of three basic functions, C_3, R, and A, and, in addition, the optical losses and electronics system gain. As far as the optical losses are concerned, one must design the system such that the product of the Raman intensity, area of the receiving mirror and efficiency of the receiving optics (e.i., lenses, spectrograph, filters, etc.) is greater than the minimum detectable signal, where the minimum detectable signal is defined as the signal for which the signal-to-noise ratio is equal to 1. Thus, if the noise signal is minimized, the detectable signal can be proportionately decreased. In general, the signal-to-noise ratio of a photodetector can be represented for a single pulse by

$$\frac{S}{N} = \frac{i_s^2}{2e\Delta f(i_s + i_d + i_b)} \tag{14}$$

where the currents are average values. Depending on the magnitude of each of the contributing sources of noise, the detectors are known as photon, background or dark current limited.

Since the signal-to-noise ratio can be improved by averaging over a number of pulses, one would tend to design the equipment on a repetitive basis, that is, multipulse operation. In that case Equation (12) can be written

$$\frac{S}{N} = \frac{n_p i_s^2}{2e\Delta f(i_s + i_d + i_b)} \tag{15}$$

This equation would indicate that by increasing the number n of averaged pulses, any signal-to-noise ratio is possible to achieve. This is, of course, limited by the averaging time one can use, and the signal processing electronics. Since, in most modern photomultipliers the dark currents are very small (10^{-1}), the limiting noise is the background current, i_B.

In order to detect a signal, the signal-to-noise ratio must be larger than $(S/N)_{min}$. Defining the phototube sensitivity S_{ph} by

$$i_s = S_{ph} \cdot P_s \quad \text{and} \quad i_B = S_{ph} P_b \tag{16}$$

and using Equation (15) the signal power must be greater than

$$P_s \geqslant \frac{2e \frac{\Delta f}{n} \left(\frac{S}{N}\right)_{min}}{S_{ph}} \tag{17}$$

for photon limited operation and

$$P_s \geqslant \frac{\left[2e \frac{\Delta f}{n} \left(\frac{S}{N}\right)_{min} i_B\right]^{\frac{1}{2}}}{S_{ph}} \tag{18}$$

for background limited operation. Equation (18) indicated that for daytime operation the required scattered power or signal power must be larger than for night-time operation.

As mentioned previously, C_3 is a quantity associated with the molecular invariants of the specie under investigation and is, therefore, a constant for each specie of interest. Some of these molecular invariants are listed in References 10 and 11. Figure 8 represents a plot of the behavior of the expression $\mathcal{R}$ as a function of the Raman shift for a nitrogen and ruby laser as the illuminating sources. It is quite evident from this figure that the scattered intensity not only decreases with the increase in the Raman frequency shift of a given specie, but also that the decrease in intensity is more pronounced for the lower frequency primary radiation source.

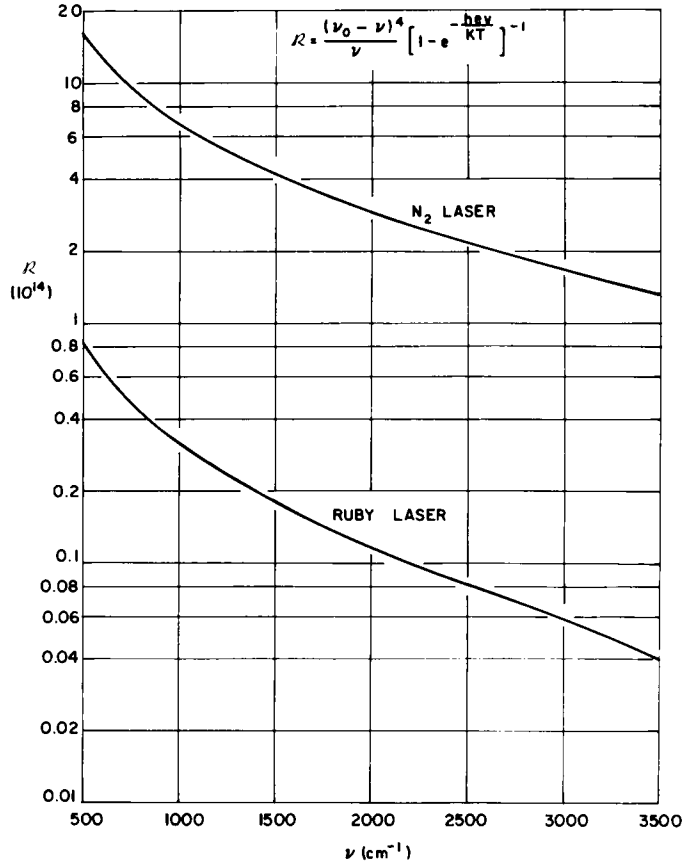

Figure 8. Raman scattering coefficient as a function of the Raman shift, for ruby and nitrogen laser as the illumination.

Whereas the value of $\mathcal{R}$ for the N_2 laser decreases by a factor of about 15 for a Raman shift between 500 and 3500 cm^{-1}, it decreases by a factor of about 30 for a ruby laser for the same Raman shift interval. This fact, in addition to the fourth power dependence of the intensity of the scattered radiation on the illuminating frequency makes it desirable to move the primary source of radiation into the u.v. region. There are, however, limitations on the usable frequency imposed not only by the scarcity of high intensity sources in this region, but also by the increase of the scattering coefficient at these frequencies, which enormously increases the atmospheric attenuation of the scattered signals received. This is evident from Figures 5 and 6, where the scattering coefficient β, as a function of wavelength, is plotted, and from Figure 9 where the attenuation of the Raman signal for several species as a function of distance are compared for

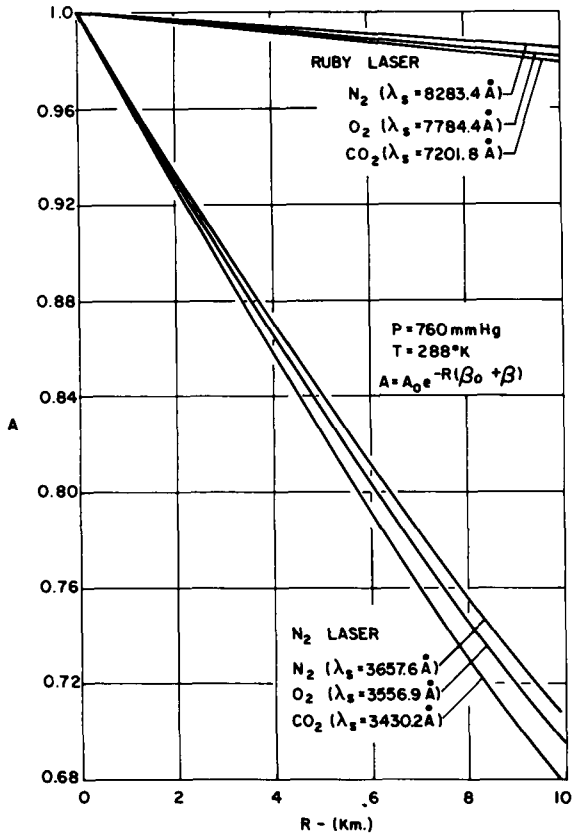

Figure 9. Atmospheric attenuation of Raman scattered radiation from several species as a function of distance.

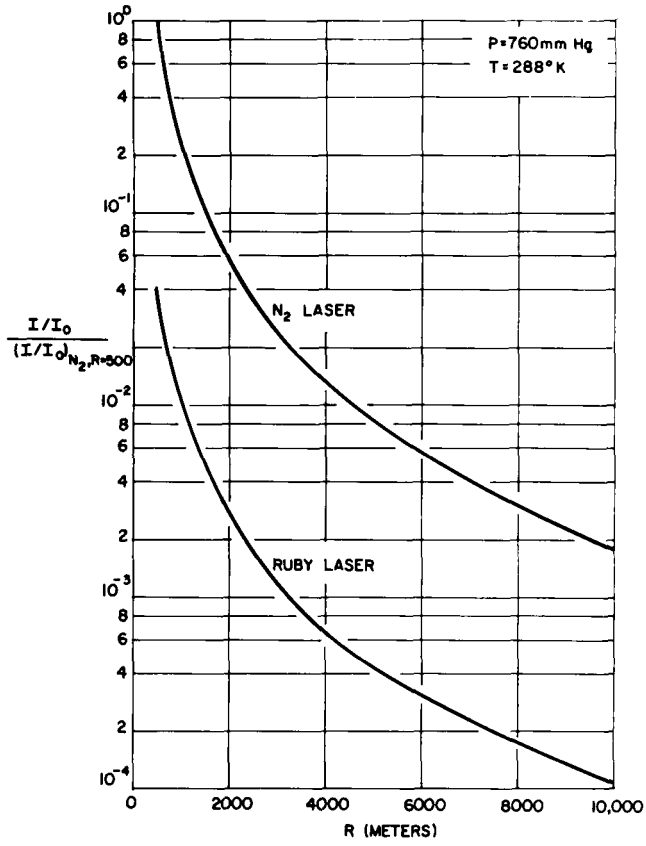

Figure 10. Raman intensity for O_2 as a function of distance. Normalized by the relative Raman intensity of a N_2 laser at 500m.

an N_2 laser at (3371Å) and a ruby laser at (6943Å) as the primary illuminating source. The results of Figures 8 and 9 clearly counteract each other. While a higher frequency source is indicated from the point-of-view of the fourth power relationship for the scattered radiation, a lower frequency is indicated from the point-of-view of attenuation.

In Figure 10, the relative intensity of a Raman signal obtainable using a nitrogen and a ruby laser is shown. An inspection of this figure indicates clearly that the overriding feature here is still the fourth power dependence of the scattered radiation on the frequency. With the increasing distance of the scattering sample, the attenuation at higher frequencies increases and eventually becomes dominant. For example, at about 25 km the relative intensity of the scattered radiation for the ruby laser becomes larger than the one for the N_2 laser. One must note that the intensity in Figure 10

was obtained on the assumption that the primary intensities of both lasers were equal. As is well-known, at the present time, ruby lasers capable of delivering several hundred megawatts in a single pulse operation are available as standard off-shelf units, while nitrogen lasers of only several hundred kilowatts can be commercially obtained. For this reason, in some applications it might be advantageous to use a ruby laser with its lower radiation frequency, rather than a nitrogen laser with its higher operating frequency. The choice of the mode of operation, that is, single pulse or repetitive, would greatly influence the choice of the laser. Whereas a nitrogen laser is capable of operating at a rate of several hundred pulses/second, a ruby laser is capable of a single pulse or, at most, several pulses/minute operation. Consistent with the requirements for an improved signal resolution as indicated above, the multipulse operation possible with the nitrogen laser is indicated. However, this kind of operation would provide a time average signal.

While it might be advantageous for a number of reasons to operate at a higher frequency in certain applications, other considerations could result in the choice of lower operating frequencies. An inspection of Figure 10 or Table 5 and Table 6 reveals that from the point-of-view of signal strength at short distances the N_2 laser is superior, providing a laser of appropriate power is available. If, however, one is interested in field monitoring of some particular species, a size reduction of the apparatus would be desirable. Replacement of the spectrometer with filters would require a better line separation of the Raman scattered radiation. As evident from Table 6, a lower operating frequency provides better line separation. While, for example, the line separation of NO from O_2 is 40.9Å with a nitrogen laser, it is 98.1Å for a ruby laser. The wider line separation when using a lower frequency illuminating source (ruby) permits the utilization of filters of reasonable bandpass. This feature in conjunction with the higher pulse power available could, in certain cases, be advantageous. In discussing the choice of frequency one must mention the possibility of using a variable frequency illuminating source. This kind of source might enable one to

Table 5. Equivalent Raman Scattering Cross-Section

	Ruby	*N_2*
O_2	$4.72 \cdot 10^{-30}$	$1.08 \cdot 10^{-28}$
N_2	$2.85 \cdot 10^{-30}$	$7.47 \cdot 10^{-29}$
CO_2	$6.57 \cdot 10^{-29}$	$1.45 \cdot 10^{-27}$
NO	$7.2 \cdot 10^{-31}$	$3.2 \cdot 10^{-29}$

Table 6. Raman Wavelength of Some Molecules Corresponding to Ruby and N_2 Lasers as Primary Illuminators

	λ_s [Å] *Ruby Laser*	λ_s *N_2 Laser*
NO	7982.5	3597.8
SO_2	7546.2	3506.4
	7201.8	3430.2
	7668.0	3532.5
NO_2	7643.3	3527.2
	7324.2	3457.7
	7821.4	3564.7
H_2O	9305.5	3844.1
	7807.4	3561.8
	9392.1	3858.8
CO_2	7683.5	3535.8
	7623.4	3523.0
CO	8156.8	3632.8
N_2	8283.4	3657.6
O_2	7784.4	3556.9

utilize the so-called resonance Raman scattering, which is capable of providing scattered signals several orders of magnitude higher than the normal Raman scattering.

Finally, the question of eye safety must be considered in choosing a laser for air pollution monitoring. In his respect, the higher frequency N_2 laser might be considered safer than the lower frequency ruby laser. It should be mentioned here that exposure to laser radiation may cause two major injuries to the human eye. These are u.v. photokeratitis and retinal injury. While photokeratitis might be very painful, it is generally not a permanent injury. Retinal injury, however, is generally irreversible and may result in permanent visual impairment. While photokeratitis is a result of irradiation of the external tissues of the eye, retinal injuries are caused by radiation transmitted through the lens and vitreous fluid of the eye. It is generally assumed that the high frequency limit of ocular transmission is at about 25000 cm^{-1}. This limit, however, is not absolute. There might still be some transmission at this or high frequency to cause injury, in particular, at high power densities and direct, close observation. The opacity of the eye to high frequency radiation again suggests the superiority of the N_2 laser over the ruby laser. In any case, provisions must

be made to avoid direct or indirect exposure to the intense radiation in question.

The choice of the laser will thus have to be made in each case consistent with the given application and with the proper consideration of the previously indicated pro and con features.

From the above considerations, it may be concluded that an air pollution monitoring and measuring apparatus can be constructed which would consist essentially of the following major components:

1. A high powered laser source capable of stimulating Raman scattering at a remote sample.
2. A high powered telescope capable of receiving radiation from a remote source.
3. A spectroscope or narrow bandpass filter capable of sorting and transmitting the different signals received.
4. Signal processing and recording system.

The last component of the pollution monitor consists of a photomultiplier tube power supply and electronic processing and recording equipment. The complexity of the system depends on the applications intended. In Figure 11, a block diagram in its most general form of a possible monitoring station is shown.

Figure 12 shows a photographic view of an experimental apparatus constructed in our laboratory. This apparatus uses a Q-switched ruby laser capable of delivering a pulse of 100 megawatt peak power. The pulse duration of 10 nanoseconds is sufficiently short to permit a relatively good depth resolution. The receiving telescope consists of a 30 cm diameter parabolic mirror of 3.6m focal length. The system utilizes a Jarrel Ash 1/2m monochrometer terminated by a RCA 8853 photomultiplier. The signal can be directly recorded on an oscilloscope or processes by the electroatomic data processing equipment as seen in the photograph. The whole system is mounted on a movable platform where angle and elevation can be adjusted.

While the ideal mounting of the transmitting and receiving optics would be concentric as indicated diagramatically in Figure 13, this experimental apparatus was constructed utilizing the available equipment and due to this lack of an appropriate Cassegrainian mirror, is not concentric. As indicated above, there are a number of difficulties associated with correlating the received signal and the actual specie concentration at a given range. These may change from day-to-day or hour-to-hour according to the atmospheric conditions, time of day and season of the year. To overcome these difficulties, a parallel channel is generally introduced which is monitoring a known component of the atmosphere, and normalizing the measured specie

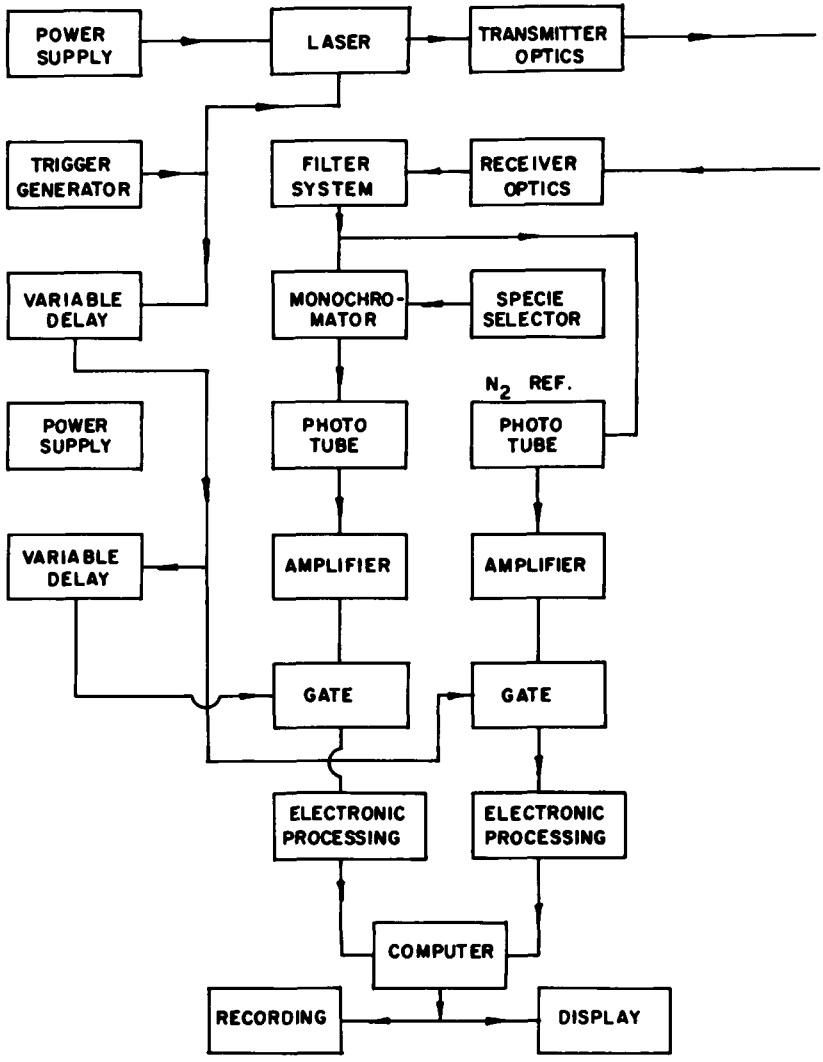

Figure 11. Tentative block diagram of a remote air pollution monitor.

with respect to this component. This known monitored component may be nitrogen. This channel is indicated diagramatically in Figure 13. In case of a single pulse operation, the received signal can be processed using a beam splitter and two separate photon processing channels. In multipulse operation the same procedure may be followed or a single photon

Figure 12. Photographic view of the experimental apparatus in the laboratory.

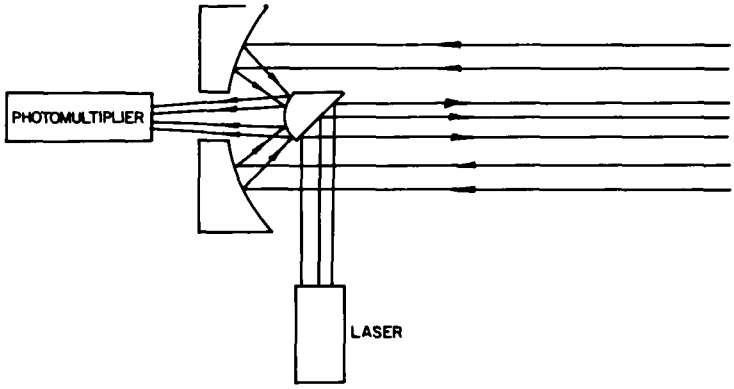

Figure 13. Concentric configuration of transmitter and receiver.

processing channel may be employed and the sampling can be alternated between N_2 and the specie of interest.

Concluding Remarks

It is quite evident from the above discussions that a pollution monitoring measuring and detection device utilizing the Raman effect could be constructed. While short distance, remote, single-ended measurements of pollutants of high concentration can be made at present with the available shelf equipment, low concentrations of particular species at greater distances might require further developments not only in lasers, photomultipliers and processing electrons, but also in the field of the so-called "Resonant Raman Effect." The resonant Raman effect provides signals several orders of magnitude higher than the normal Raman effect. These could effectively increase the sensing distance or decrease the concentration of the pollutant species, without adversely affecting the minimal signal-to-noise ratios required.

REFERENCES

1. Air Conservation Publication No. 80 of the American Assoc. for the Advancement of Science, Washington, D.C., 1965.
2. *Cleaning Our Environment*, A report of the American Chemical Society, Washington, D.C., 1969.
3. G. Herzberg, *Infrared and Raman Spectra of Diatomic Molecules,* D. Van Nostrand Co., Inc., New York, 1945.
4. G. Herzberg, *Infrared and Raman Spectra of Polyatomic Molecules,* D. Van Nostrand Co., Inc., New York, 1945.
5. L. R. Kohler, *Ultraviolet Radiation,* John Wiley and Sons, Inc., New York, 1965.

6. S. Lederman, Molecular Spectra and the Raman Effect, A Short Review, Polytechnic Institute of Brooklyn, PIBAL Report No. 71-15, 1971.
7. S. I. Mizushima, Raman Effect, *Handbuch der Physik*, XXVI, Springer-Verlag, 1958.
8. W. K. Pratt, *Laser Communications Systems*, John Wiley and Sons, Inc., New York, 1969.
9. G. F. Widhopf and S. Lederman, Specie Concentration Measurements Utilizing Laser Induced Raman Scattering, *AIAA J.*, 9(2), 309-316, 1971.
10. H. W. Schrotter and H. J. Bernstein, Intensity in the Raman Effect, Absolute Intensities for Some Gases and Vapors, *J. Molecular Spectroscopy*, **12**, 1-17, 1964.
11. E. J. Stansbury, M. F. Crawford, and H. L. Welsh, Determination of Rates of Change of Polarizability from Raman and Rayleigh Intensities, *Canadian J. of Physics*, **31**, 1953.